THE JOURNAL OF PHYSICAL CHEMISTRY B LETTERS

2007, *111,* 9702−9705
Published on Web 08/02/2007

On the Possibility of Extending the Noro−Frenkel Generalized Law of Correspondent States to Nonisotropic Patchy Interactions

Giuseppe Foffi*,‡ and Francesco Sciortino†

Institut Romand de Recherche Numérique en Physique des Matériaux (IRRMA) and Institute of Theoretical Physics (ITP), Ecole Polytechnique Fédérale de Lausanne (EPFL), CH-1015 Lausanne, Switzerland, and Dipartimento di Fisica and INFM-CNR-CRS Soft, Università di Roma La Sapienza, P.le A. Moro 2, 00185 Roma, Italy

Received: June 1, 2007; In Final Form: July 19, 2007

Colloidal systems (and protein solutions) are often characterized by attractive interactions whose ranges are much smaller than the particle size. When this is the case and the interaction is spherical, systems obey a generalized law of correspondent states (GLCS), first proposed by Noro and Frenkel (Noro, M. G.; Frenkel, D. *J. Chem. Phys.* **2000**, *113*, 2941). The thermodynamic properties become insensitive to the details of the potential, depending only on the value of the second virial coefficient B_2 and the density ρ. The GLCS does not generically hold for the case of nonspherical potentials. In this Letter, we suggest that when particles interact via short-ranged small-angular amplitude patchy interactions (so that the condition of only one bond per patch is fulfilled), it is still possible to generalize the GLCS close to the liquid−gas critical point.

In colloidal and in protein systems, the interaction potential is often short-ranged, that is, small as compared to the particle size. The small-range interaction brings some peculiar behavior both to the system thermodynamics and on the dynamics. For example, the gas−liquid phase separation becomes metastable with respect to crystallization[1] (and hence, a proper equilibrium liquid phase is missing). In addition, for very short ranges, the kinetic arrest (glass) line becomes reentrant, and two different glass phases appear.[2,3] The presence of short-range attractions is also invoked to explain the so-called "crystallization slot" in the phase diagram of globular proteins.[4]

A common property unifies all spherically symmetric short-ranged attractive potentials, independently from their actual shape. Indeed, Noro and Frenkel[5] showed that the thermodynamical properties of systems interacting with short-range attractive potentials are all equivalent if scaled by the proper variables, that is, they obey a generalized law of correspondent stated (GLCS). They showed that the virial coefficient can be used as a scaling variable for the strength of the interaction. Recently, the GLCS has been shown to arise from the fact that, due to the short range of the interaction, each interacting pair of particles (a bond) contributes independently and equally to the partition function.[6]

The above considerations are valid for centrosymmetric potentials and cannot be straightforwardly extended to nonspherical cases,[7,8] that is, when interactions are patchy and strongly directional. In the case of molecular fluids, patchy interactions are relevant in network-forming systems, like silica[9,10] and water[11,12] and in all associating fluids[13,14] in which the hydrogen bond plays an important role. For colloidal systems, this interest is justified by recent advances in the synthesis and characterization of patchy particles[15−18] or functionalized colloidal particles.[19] For what concerns proteins, it is well-established that the interactions are intrinsically directional[20−22] and that their description in terms of isotropic potentials represents only a first-order approximation.

Recent progress in understanding the thermodynamics of patchy colloidal particles has been based on application of the thermodynamical perturbation theory developed by Wertheim.[23] The theory, which does not account for the geometry of the patches, assumes that each patch acts as an independent interacting unit. In addition, the theory neglects the possibility of the closed loops of bonds. Despite these approximations, several predictions of the theory have been numerically confirmed.[13,24,25] It has been shown that (for the case of patchy interactions) the number of independent interacting patches (the valence) is the key ingredient in controlling the phase diagram of the system. Upon lowering the valencey, the liquid−gas critical point shifts to smaller and smaller densities so that liquid states of vanishing density (empty liquids) become accessible.[24] The Wertheim expression for the bonding free energy is a function only of the bond probability and of the valencey. In this respect, the theory suggests that systems with the same valencey should behave similarly if the bond probability is the same. Since the bond probability is related to the chemical bonding constant[13,25] and since, for large attraction strengths, the chemical constant is proportional to the second virial coefficient,[26] the Wertheim theory suggests that universality based on the virial scaling can be recovered also in the case of patchy interactions when valencey is preserved.

To address the issue of a possible generalization of the Noro−Frenkel scaling, we have extended the investigation concerning the location of the critical point for the patchy model introduced by Kern and Frenkel[7] for several values of the attraction range and of the width of the patchy attractive region. The choice of this potential is motivated by the fact that angular and radial

‡ Ecole Polytechnique Fédérale de Lausanne (EPFL).
† Università di Roma La Sapienza.

10.1021/jp074253r CCC: $37.00

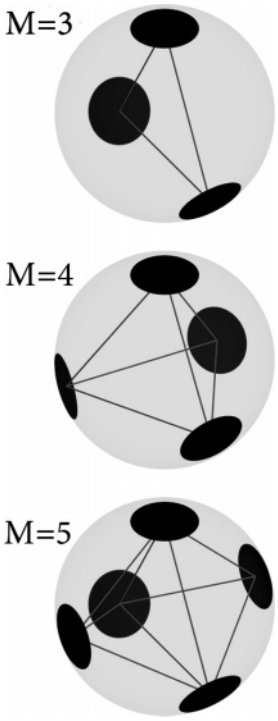

Figure 1. Pictorial representation of the three different patch geometries considered in this work. The solid angle of each patch is $2\pi(1 - \cos\theta)$, where θ is the cone semi-angle.

properties can be independently modified. More precisely, the two-body potential is defined as

$$u(\mathbf{r}_{ij}) = u^{sw}(r_{ij})f(\{\Omega_{ij}\}) \quad (1)$$

where $u^{sw}(r_{ij})$ is an isotropic square-well term of depth u_0 and attractive range $\sigma + \Delta$ and $f(\{\Omega_{ij}\})$ is a function that depends on the orientation of the two interacting particles $\{\Omega_{ij}\}$. The diameter of the particles and the depth of the square well have been chosen as units of length and energy respectively, that is, $\sigma = 1$ and $u_0 = 1$. Each particle is characterized by M identical patches. A patch α is defined as the intersection of the surface of the sphere with a cone with a half-opening angle θ that has the vertex in the center of the particle and the axis directed toward the direction $\hat{\mathbf{u}}_\alpha$. The angular function $f(\{\Omega_{ij}\})$ is defined as

$$f(\{\Omega_{ij}\}) = \begin{cases} 1 \text{ if} \begin{cases} \hat{\mathbf{r}}_{ij}\cdot\hat{\mathbf{u}}_\alpha > \cos\theta & \text{some patch } \alpha \text{ on particle } i \\ \text{and} \\ \hat{\mathbf{r}}_{ij}\cdot\hat{\mathbf{u}}_\beta > \cos\theta & \text{some patch } \beta \text{ on particle } j \end{cases} \\ 0 \text{ else} \end{cases} \quad (2)$$

where $\hat{\mathbf{r}}_{ij}$ is the direction of the versor that joins the centers of the two interacting particles and $\alpha(\beta)$ some patch belonging to the particle $i(j)$. In practice, two particles interact attractively if, when they are within the attractive distance $\sigma + \Delta$, two patches are properly facing each other. When this is the case, the two particles are considered bonded. Decreasing Δ reduces the range of the attraction, whereas reducing θ diminishes the angular size of the patches. In the limit $\Delta \to 0$, the model goes toward the patchy Baxter limit. In the limit $\cos\theta \to 1$, the patch goes to the point limit.

In the present work, we focus on M = 3, 4, and 5 patches, located on the surface of the particle, as shown in the cartoon of Figure 1. Different from previous studies,[7] we consider values of Δ and θ such that, due to steric reasons, each patch is involved simultaneously in only one pair interaction, that is, those values fulfilling the condition $\sin\theta > \sigma^2/[2(\sigma+\Delta)^2]$. Under this single-bond-per-patch condition, the number of patches coincides also with the maximum number of possible bonds per particle.

TABLE 1: Critical Point Properties for All Studied Models, Labeled by the Values M, Δ, and $\cos\theta$[a]

M	Δ	$\cos\theta$	T_c	ρ_c	p_b^c	B_2^c/B_2^{HS}
3	0.050	0.92	0.1076	0.151	0.727	−23.67
3	0.070	0.92	0.1113	0.150	0.732	−24.92
3	0.119	0.92	0.1180	0.134	0.721	−26.71
3	0.119	0.895	0.1252	0.136	0.737	−28.29
3	0.119	0.92	0.1180	0.134	0.721	−26.71
3	0.119	0.95	0.1069	0.131	0.726	−25.13
3	0.119	0.97	0.0968	0.129	0.726	−23.92
4	0.010	0.92	0.1140	0.326	0.656	−4.02
4	0.050	0.92	0.1392	0.306	0.652	−4.32
4	0.070	0.92	0.1468	0.306	0.641	−4.24
4	0.090	0.92	0.1511	0.289	0.642	−4.65
4	0.119	0.92	0.1573	0.276	0.644	−4.92
4	0.119	0.895	0.1682	0.267	0.635	−5.74
4	0.119	0.92	0.1573	0.276	0.644	−4.92
4	0.119	0.94	0.1484	0.307	0.667	−3.85
5	0.010	0.92	0.1259	0.393	0.567	−2.41
5	0.050	0.92	0.1570	0.387	0.588	−2.67
5	0.070	0.92	0.1653	0.374	0.585	−2.81
5	0.090	0.92	0.1723	0.362	0.581	−2.90
5	0.119	0.92	0.1808	0.348	0.577	−3.03
5	0.119	0.895	0.1959	0.333	0.570	−3.53
5	0.119	0.92	0.1808	0.348	0.577	−3.03
5	0.119	0.95	0.1601	0.372	0.589	−2.22

[a] The different columns indicate the critical temperature T_c, critical density ρ_c, the bond probability p_b^c, and the reduced value of the second virial coefficient B_2^c/B_2^{HS} at the critical point. The estimated errors for each of these quantities are $\pm 0.0005(T_c)$, $\pm 0.007(\rho_c)$, and $\pm 0.005(p_b^c)$. The error in B_2 arises from the error in T_c and differs for each point due to the nonlinear relation between B_2 and T. The field-mixing parameter s is always smaller than 0.08.

The Kern−Frenkel potential possess an analytical expression for the second virial coefficient

$$\frac{B_2}{B_2^{HS}} = 1 - \chi^2((1+\Delta)^3 - 1)(e^{1/T} - 1) \quad (3)$$

where $\chi = M[(1 - \cos(\theta))/2]$ is the percentage of surface covered by the attractive patches and the temperature is measured in reduced units, that is, $k_B = 1$. Here, B_2^{HS} is the hard-sphere component of the virial coefficient. To calculate the location of the gas−liquid critical point, we perform grand canonical Monte Carlo (GCMC) simulations,[27] complemented with histogram reweighting techniques to match the distribution of the order parameter $\rho - se$ with the known functional dependence expected at the Ising universality class critical point.[28] Here, e is the potential energy density, ρ is the number density, and s is the mixing field parameter. We did not performed a finite size study since we were only interested in the trends with the range Δ and the angular size of the patches θ. We have studied systems of size $L = 6$ for $M = 4$ and 5 and $L = 7$ for $M = 3$, where L is the side length of the cubic simulation box. For each studied M, using the methods described in ref 29, we calculated the critical temperature T_c and density ρ_c for values of Δ between 0.119 and 0.01 (at fixed $\cos\theta = 0.92$) and for $\cos\theta$ between 0.895 and 0.99 (at fixed $\Delta = 0.119$). The results are summarized in Table 1.

We start by analyzing the results as a function of Δ, at fixed $\cos\theta = 0.92$. Figure 2 shows that T_c decreases with Δ, while

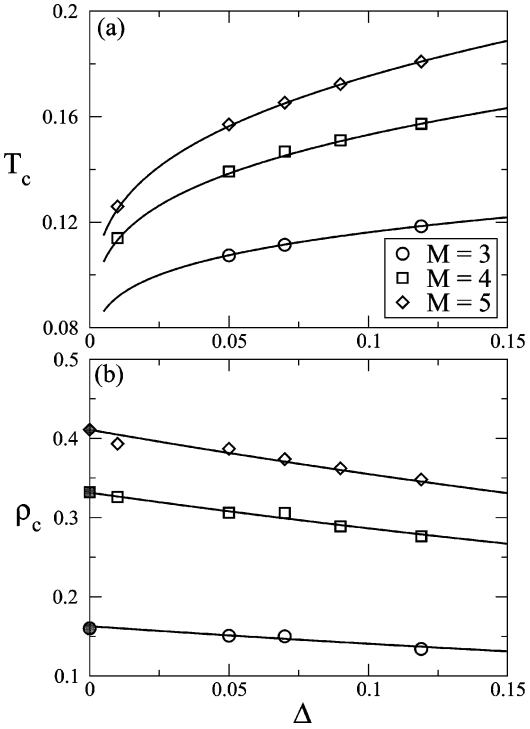

Figure 2. Critical temperature T_c (a) and critical density ρ_c (b) as a function of the range Δ, at fixed patch angular size cos $\theta = 0.92$. Lines in (a) correspond to constant values of B_2, specifically $B_2/B_2^{HS} = -3.03$ for $M = 5$, $B_2/B_2^{HS} = -4.92$ for $M = 4$, and $B_2/B_2^{HS} = -26.71$ for $M = 3$. Lines in (b) are $\rho_c(\Delta) = \rho_c(0)/(1 + 0.5\Delta)^3$, where $\rho_c(0)$ (shaded point) is a fitting parameter. The fit values are $\rho_c(0) = 0.41$ for $M = 5$, $\rho_c(0) = 0.33$ for $M = 4$, and $\rho_c(0) = 0.16$ for $M = 3$. Open symbols are simulation results.

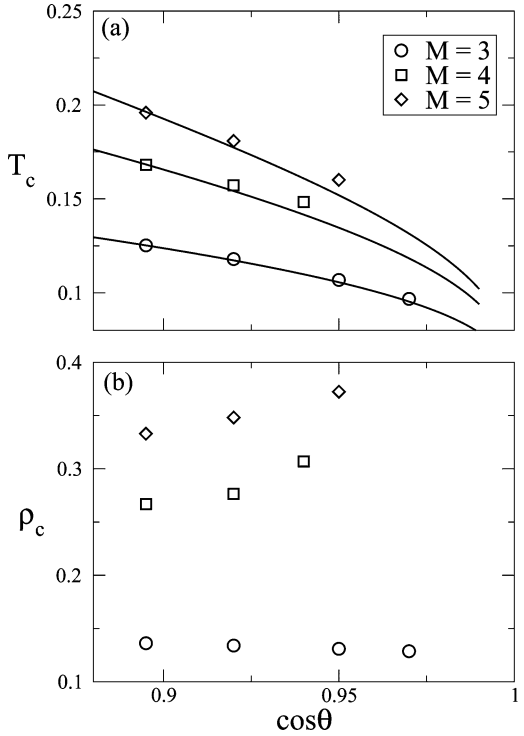

Figure 3. Critical temperature T_c (a) and critical density ρ_c (b) as a function of the angular patch size cosθ, at fixed range $\Delta = 0.119$. Lines in (a) correspond to constant values of B_2, specifically $B_2/B_2^{HS} = -3.53$ for $M = 5$, $B_2/B_2^{HS} = -5.74$ for $M = 4$, and $B_2/B_2^{HS} = -28.29$ for $M = 3$. Open symbols are simulation results.

ρ_c increases. The Δ dependence of ρ_c can be conveniently described by $\rho_c(\Delta) = \rho_c(0)/(1 + 0.5\Delta)^3$, a functional form which suggests that ρ_c would be constant if measured using the average distance between two bonded particles $(1 + 0.5\Delta)$ as the unit of length. The resulting $\rho_c(0)$-extrapolated value provides an estimate of the corresponding patchy Baxter model ρ_c. Figure 2a shows also that the T_c dependences are apparently well described by iso-B_2 lines. Each M is characterized by a different B_2 value, enforcing the existence of a GLCS for each valence. As a confirmation, we evaluate the values of B_2^c/B_2^{HS} at the critical point for the patchy particle model studied in ref 24. The resulting values for $M = 3$, 4, and 5 are respectively $B_2^c/B_2^{HS} = -28.12$, -4.95, and -2.78, very similar to the values reported in the present study. We also note that the B_2^c differences between different M values are much larger than the variation with Δ at constant M. Hence at a zeroth-order approximation, when the repulsive part of the potential is complemented by localized patchy interactions, B_2 can be considered as a scaling variable of a GLCS in the single-bond-per-patch condition.

A closer look at the actual B_2 values (see Table 1) shows that a small trend in the B_2 values is present, which is hidden in the logarithmic transformation relating B_2 to T (see eq 3). Still, the B_2 differences between different M values are much larger than the variation with Δ at constant M. This suggests that, at a zeroth-order approximation, B_2 can be considered as a scaling variable of a GLCS in the single-bond-per-patch condition. Thus, provided that the geometry of the patches is such that their number coincides with the maximum valencey, B_2 carries the information on the valencey of the patchy interaction potential. These results suggest that, statistically, configurations with the same Boltzmann weight are generated under an isotropic scaling (to change the interparticle distances preserving the same bonding pattern) and a simultaneous change of both Δ and T such that B_2 remains constant. It is interesting to observe that the GLCS for the isotropic square well is fulfilled for values of the range smaller than 0.05,[6,30] whereas for the three models discussed here, GLCS appears to hold for longer ranges.

Figure 3 shows T_c and ρ_c, this time at $\Delta = 0.119$, as a function of cos θ. For values of cos θ larger than the one reported in the figure, crystallization is observed within the simulation time, preventing the possibility of evaluating the critical parameters. This effect suggests that the liquid−gas critical point is metastable, as in the case of spherical short-range potentials. The observation of crystallization informs us already that upon reducing θ, some bonding patterns acquire a larger statistical weight. Indeed, different from the previous case, small deviations from a GLCS are observed in T (see lines Figure 3a) and not only in B_2^c. We attribute these deviations to the fact that by changing the angular part of the potential, the statistical relevance of specific bonding patterns varies. In other words, it is not possible to vary the orientation of the particles to preserve the bonding upon changing θ, that is, it is not possible to perform the operation equivalent to rescaling the distances to preserve the bonding pattern upon changing Δ. We expect that the breaking of the scaling will be enhanced at state points far from the critical region where an extensive bonding pattern is present, that is, low T and large ρ. Concerning the θ dependence of ρ_c, we note that it increases with cos θ for the cases $M = 5$ and 4, while it weakly decreases for $M = 3$. We have no clear arguments for interpreting the $\rho_c(\theta)$ trends, except for the fact that the observed dependence (more significant for $M = 4$ and 5) suggests a nontrivial coupling between the angular correlation induced by bonding and the density. For these two M values,

small bonding angles appear to require smaller average distances between next-nearest neighbor particles, implying larger densities.

The argument behind the quasi-validity of the GLCS for each M class is based on the fact that the relevant role is played by the bonding pattern,[6] which is supposed to be statistically identical for all members of the class along corresponding states. Hence, the number of bonds at the critical point should be similar. To double check this statement, we also report in Table 1 the bond probability p_b^c, defined as the potential energy at the critical point normalized by the energy of the fully bonded system. Such a quantity is indeed constant for each M value, in agreement with (and strongly supporting) the possibility of defining a different GLCS for each valencey class. We also note that, within each M class, the variations of p_b^c are smaller than the one of B_2, suggesting that the bond probability may result in a better scaling variable that of than B_2. A small trend in p_b^c is only observed in the θ dependence. We also note that this observation is in agreement with the Wertheim theory[23] and with the identification of the bond free energy as the appropriate scaling variable for the spherical case.[6]

In summary, we have provided evidence that different short-ranged nonspherical potentials, but with the same number of single-bond patches, essentially obey a GLCS. The condition of a single-bond-per-patch requires that both the attraction range and the angular size of the patches are small. Breakdowns of the GLCS can be expected for potentials which differ in their angular part, especially for very small angular sizes ($\cos\theta \rightarrow 1$) since, in conditions of extensive bonding, the statistical weight of the closed loops of bonds becomes significantly effected by the angular patch size.

We acknowledge support from the Swiss National Science Foundation Grant No. 99200021-105382/1 (G.F.) and MIUR PRIN (F.S.).

References and Notes

(1) Gast, A. P.; Russell, W. B.; Hall, C. K. *J. Colloid Interface Sci.* **1983**, *96*, 251.

(2) Sciortino, F. *Nat. Mater.* **2002**, *1*, 145.

(3) Dawson, K. A.; Foffi, G.; Fuchs, M.; Gotze, W.; Sciortino, F.; Sperl, M.; Tartaglia, P.; Voigtmann, T.; Zaccarelli, E. *Phys. Rev. E* **2001**, *63*, 11401.

(4) ten Wolde, P. R.; Frenkel, D. *Science* **1997**, *277*, 1975.

(5) Noro, M.; Frenkel, D. *J. Chem. Phys.* **2000**, *113*, 2941.

(6) Foffi, G.; Sciortino, F. *Phys. Rev. E* **2006**, *74*, 050401.

(7) Kern, N.; Frenkel, D. *J. Chem. Phys.* **2003**, *118*, 9882.

(8) Charbonneau, P.; Frenkel, D. *J. Chem. Phys.* **2007**, *126*, 196101.

(9) Vega, C.; Monson, P. *J. Chem. Phys.* **1998**, *109*, 9938.

(10) De Michele, C.; Gabrielli, S.; Tartaglia, P.; Sciortino, F. *J. Phys. Chem. B* **2006**, *110*, 8064.

(11) Kolafa, J.; Nezbeda, I. *Mol. Phys.* **1987**, *61*, 161.

(12) De Michele, C.; Tartaglia, P.; Sciortino, F. *J. Chem. Phys.* **2006**, *125*, 204710.

(13) Chapman, W.; Jackson, G.; Gubbins, K. *Mol. Phys.* **1988**, *65*, 1057.

(14) Sear, R.; Jackson, G. *J. Chem. Phys.* **1996**, *105*, 1113.

(15) Manoharan, V.; Elsesser, M.; Pine, D. *Science* **2003**, *301*, 483.

(16) Cho, Y.-S.; Yi, G.-R.; Lim, J.-M.; Kim, S.-H.; Manoharan, V.; Pine, D.; Yang, S.-M. *J. Am. Chem. Soc.* **2005**, *127*, 15968.

(17) Zerrouki, D.; Rotenberg, B.; Abramson, S.; Baudry, J.; Goubault, C.; Leal-Calderon, F.; Pine, D.; Bibette, J. *Langmuir* **2006**, *22*, 57.

(18) Zhang, G.; Wang, D.; Möhwald, H. *Angew. Chem., Int. Ed.* **2005**, *44*, 1.

(19) Mirkin, C.; Letsinger, R.; Mucic, R.; Storhoff, J. *Nature* **1996**, *382*, 607.

(20) Sear, R. P. *J. Chem. Phys* **1999**, *111*, 4800.

(21) Lomakin, A.; Asherie, N.; Benedek, G. B. *Proc. Natl. Acad. Sci. U.S.A.* **1999**, *96*, 9465.

(22) Liu, H.; Kumar, S. K.; Sciortino, F. *J. Chem. Phys.* In press.

(23) Wertheim, M. *J. Stat. Phys.* **1984**, *35*, 19.

(24) Bianchi, E.; Largo, J.; Tartaglia, P.; Zaccarelli, E.; Sciortino, F. *Phys. Rev. Lett.* **2006**, *97*, 168301.

(25) Sciortino, F.; Bianchi, E.; Douglas, J. F.; Tartaglia, P. *J. Chem. Phys.* **2007**, *126*, 194903.

(26) Sear, R. P. *Curr. Opin. Colloid Interface Sci.* **2006**, *11*, 35.

(27) Frenkel, D.; Smit, B. *Understanding Molecular Simulation*, 2nd ed.; Academic Press: London, 2001.

(28) Wilding, N. *J. Phys.: Condens. Matter* **1997**, *9*, 585.

(29) Romano, F.; Tartaglia, P.; Sciortino, F. *J. Phys.: Condens. Matter* **2007**, *19*, 322101.

(30) Malijevský, A.; Yuste, S.; Santos, A. *J. Chem. Phys.* **2006**, *125*, 074507.